Three-Dimensional Binary Superlattices of Oppositely Charged Colloids

Paul Bartlett and Andrew I. Campbell
School of Chemistry, University of Bristol, Bristol BS8 1TS, United Kingdom
(Received 29 April 2005; published 16 September 2005)

We report the equilibrium self-assembly of binary crystals of oppositely charged colloidal microspheres at high density. By varying the magnitude of the charge on near equal-sized spheres we show that the structure of the binary crystal may be switched between face-centered cubic, cesium chloride, and sodium chloride. We interpret these transformations in terms of a competition between entropic and Coulombic forces.

DOI: 10.1103/PhysRevLett.95.128302 PACS numbers: 82.70.Dd, 05.70.Fh, 81.16.Dn

The spontaneous crystallization of mixtures of large and small colloids continues to fascinate material scientists since the first observation of colloidal alloys, over two decades ago [1]. There are several reasons for this continuing interest: From a fundamental standpoint, colloids provide arguably the best experimental realization of the hard-sphere model, whose phase diagram is completely dominated by entropy. Consequently, the rich variety of self-assembly phenomena seen in colloidal mixtures provides a fascinating test bed for many-body statistical physics. From a practical standpoint, colloidal assembly has great technological potential as a fabrication technique for three-dimensional photonic band gap (PBG) materials [2], ultrafast optical switches [3], and chemical sensors [4]. Most studies of colloidal assembly have, to date, been restricted to the simplest situation, that of purely repulsive spherical particles where the particles bear either no or similar surface charges and so behave as hard spheres. Extensive computer simulations [5,6] and experiments have located [7–11] only three equilibrium binary phases for hard spheres, AB, AB_2, and AB_{13}, isostructural with the atomic analogues NaCl, AlB_2, and $NaZn_{13}$. The small number and the essentially close-packed nature of these lattices limit the practical usefulness of colloidal assembly techniques, particularly in the search for a visible PBG material. More complex architectures could, in principle, be achieved by introducing weak reversible attractions between species or by fine-tuning the interparticle forces [12–14]. Unfortunately all attempts to date to direct the assembly of attractive binary particles have created highly disordered aggregates rather than the hoped-for crystalline structures.

In this Letter, we demonstrate how the introduction of a weak reversible attraction between unlike particles stabilizes non-close-packed superlattices, which would otherwise be entropically unfavorable. We use fluorescent confocal microscopy to follow the self-organization of a nonaqueous binary suspension of micron-sized spheres with similar diameters but carrying opposite charges. The nonpolar environment used ensures that the strength of the attraction is comparable to k_BT and all interactions remain reversible. We study the phase behavior as a function of the relative strength of the attractive and thermal interactions and find that we can tune the translational crystal symmetry from face-centered cubic (fcc) through body-centered cubic (bcc) to simple cubic (sc).

Our system consists of a binary mixture of near-identical sized colloidal poly(methyl methacrylate) (PMMA) particles [15] suspended in a nonpolar density and index-matched solvent. Particles are distinguished by containing one of two different cationic fluorescent dyes. The large spheres (component A) have a core radius of $R_A = 777$ nm and contain the orange-red fluorescent dye $DiIC_{18}$ (maximum emission at $\lambda_{em} = 565$ nm). The small spheres (component B), with a core radius of $R_B = 720$ nm, are labeled with the green fluorescent dye $DiOC_{18}$ ($\lambda_{em} = 502$ nm). The radius ratio ($\gamma = R_B/R_A$) is accordingly very close to unity ($\gamma = 0.93 \pm 0.01$). Both particles have a narrow distribution of sizes (polydispersity σ of about 4%) and individually form random hexagonal close-packed (rhcp) crystals at high densities. The volume fraction ϕ of the samples was defined relative to the hard-sphere freezing transition at $\phi_f = 0.494$. The solvent consists of a 78:22 wt % density and near-index matching mixture of cycloheptyl bromide (CHPB) and *cis*-decalin. PMMA particles dispersed in this low polarity solvent develop a small positive surface charge. The charge on each particle is controlled by the polarity of the dye used as the fluorescent label, with particles containing the polar $DiIC_{18}$ dye developing a larger charge than spheres labeled with the less polar $DiOC_{18}$ molecule. The particle charge may be reduced by increasing the Br^- ion concentration in solution [16]. Generating free Br^- by irradiating the suspension with ultraviolet light or by including a small length of ferromagnetic wire to act as a site for catalytic decomposition of cycloheptyl bromide led to a reduction in particle charge until at the point of zero charge the sign of the charge reversed and then became progressively more negative with further increases in $[Br^-]$. Charge inversion provides a useful, and to date unexplored, tool to adjust the interparticle interactions in a binary suspension. By working near the point of zero charge the size and sign of the charge on each species may be systematically controlled and the total interparticle potential ''tuned.'' The point of

zero charge is a function of the initial particle charge and so is different for $DiIC_{18}$ and $DiOC_{18}$-labeled particles. At low (or high) Br^- concentrations both particles are positive (or negative), all interactions are repulsive, and a hard-sphere model is appropriate. However, between these two limits the two spheres have opposite signs and the unlike interactions are attractive. We found that, in our system, we could achieve partial charge inversion by adding a small length of ferromagnetic wire to our suspensions. The particle charge, determined from measurements of conductivity and electrophoretic mobility, is a function of the time, t, of contact between suspension and metal. At $t = 0$ both particles are positively charged ($Z_A = +210e$, $Z_B = +100e$) while after 48 hours the charge on the $DiOC_{18}$-labeled spheres is reversed ($Z_A = +110e$, $Z_B = -40e$) and the two colloidal species are oppositely charged. Using the measured charges and an inverse screening length of $\kappa^{-1} = 400$ nm, determined from conductivity measurements, we estimate [17] the repulsive potential between unlike spheres at $t = 0$ as $\sim +5k_BT$, at contact. After 48 hours, charge inversion generates a cross attraction that is of order $\sim -3k_BT$. These estimates highlight the weak and reversible nature of the electrostatic interactions in our system.

Hard-sphere suspensions are fluid at low volume fractions but crystallize into a random hexagonal close-packed structure at volume fractions $\phi > 0.494$. Crystallization continues up to a volume fraction $\phi_g \approx 0.58$ where a glass transition suppresses further nucleation and growth. A binary mixture of hard spheres of similar sizes is expected to be little different. For the size ratio $\gamma = 0.93$ used here, computer simulations [18] and density functional calculations confirm that the two species remain mixed in both the crystal and fluid phases and that there is no phase separation. To explore the effect of the cross attraction on the phase behavior, we therefore prepared binary suspensions with equal volumes of A and B particles and volume fractions that ranged from $\phi = 0.48$, just below the freezing transition up to $\phi = 0.58$, the expected glass transition. The packing of the binary system of spheres was studied in real space with two-color fluorescence confocal microscopy. The different emission spectra of $DiIC_{18}$ and $DiOC_{18}$ dyes enable the two types of particles to be readily discriminated. A stack of 200 images, spaced by 0.16 μm vertically, was collected from a 73 μm $\times$ 73 μm $\times$ 32 μm volume containing $\sim$20 000 particles of each species. The suspension was sealed in a cylindrical glass cell of $\sim$50 μl volume which contained a short $\sim$5 mm length of ferromagnetic wire to catalyze the decomposition of CHPB and which could be agitated with a magnet to rapidly mix the sample prior to observation. No signs of attraction or repulsion between the particles and the wall were observed, suggesting the walls were uncharged.

Suspensions with total volume fractions $\phi \leq 0.487$ formed amorphous fluids with strong short-range order but no long-range correlations. An increase in volume fraction, however, led to the rapid formation of binary colloidal crystals. We found three distinct regular structures depending on the degree of charging, as characterized by the contact time t. The same sequence of phases was observed in all samples with volume fractions $0.50 \leq \phi \leq 0.56$. Weakly charged particles at high volume fractions assembled into a 12-fold coordinated substitutionally disordered rhcp crystal (Fig. 1). Computer simulations predict this to be a stable phase in hard-sphere mixtures of similar size [18]. In this structure the spheres are located at the crystal lattice sites in more or less random fashion. The lack of strong correlations between the two species is clearly evident in Fig. 1.

Increasing the magnitude of the opposite charges on each particle resulted in a completely different arrangement of large and small spheres. Figure 2(a) shows a striking two-color confocal micrograph of an AB superlattice formed in a suspension of $\phi = 0.528$ after 199 hours. Figure 2(b) depicts a crystallographic model of the superlattice built from a cesium chloride unit cell (space group SG 221). Rotation and cleavage along the {100} plane reproduced the structures observed in the confocal images. The cesium chloride structure consists of an equal number of cesium and chloride ions arranged alternately at the vertices of a body-centered cubic lattice so each particle has eight unlike neighbors. The lattice constant $a_{CsCl} = 1.741 \pm 0.003$ μm, determined from Fig. 2, equates to a crystal volume fraction of $\phi_{CsCl} = 0.67 \pm 0.01$. The maximum packing limit for a CsCl crystal formed from a mixture of similarly sized spheres ($\gamma > \sqrt{3} - 1$)

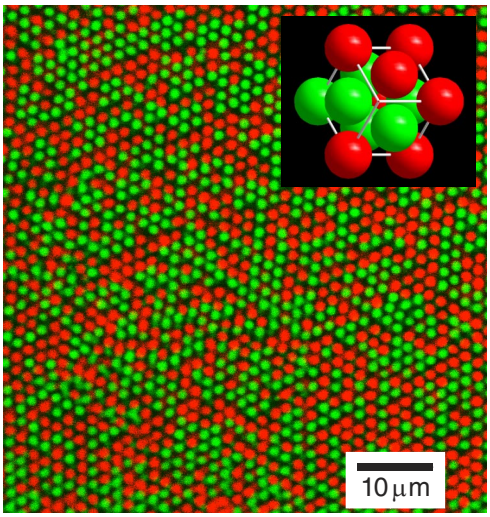

FIG. 1 (color online). Confocal image of substitutionally disordered rhcp lattice formed, after 23 hours, in a suspension with $\phi = 0.507$. The image, 8.2 μm away from a wall, depicts the close-packed {111} plane. The larger spheres (component A) are shown in green and the smaller spheres (B) in red. The inset figure shows the {111} face of a fcc unit cell of binary spheres with volume fraction $\phi_c = 0.55$.

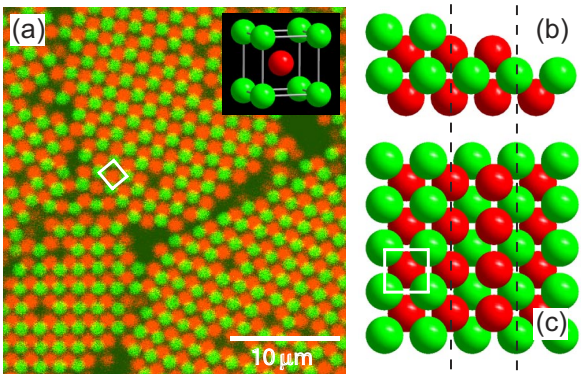

FIG. 2 (color online). Confocal image and model of cesium chloride superlattice (SG 221) formed, after 199 hours, in suspension with $\phi = 0.528$. (a) Confocal image of {100} plane in polycrystalline sample, 7.2 μm below the cover slip. Colors as in Fig. 1. Note the square lattice of A spheres around each B. Inset shows CsCl unit cell. (b),(c) Depiction of a slice through a CsCl crystal, parallel to the {100} plane, at three different depths of focus (dashed lines). (b) Projection perpendicular to {100} plane. (c) In-plane projection of {100} plane. Note the in-plane projection (c) remains unchanged as the depth of focus is stepped down through the crystal. This agrees with the experimental observation that the symmetry of the confocal image (a) does not change as the depth of focus was varied.

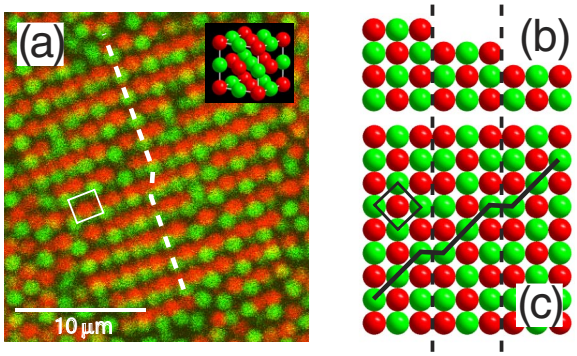

FIG. 3 (color online). Confocal image and model of sodium chloride superlattice (SG 225) formed, after 215 hours, in suspension with $\phi = 0.528$. (a) Confocal image of tilted {100} plane at a depth of 10.4 μm. Colors as in Fig. 1. Note the square lattice of A spheres around each B. Inset shows NaCl unit cell. (b),(c) Depiction of a slice through a NaCl crystal, parallel to the {100} plane, at three different depths of focus (dashed lines). (b) Projection perpendicular to {100} plane. (c) In-plane projection of {100} plane. Projection (b) reveals that the {100} plane consists of vertical columns of alternate A and B spheres. Focusing down through the {100} plane (c) causes a shift in the 2D square lattice of the face (shown in black) and a corresponding kink in the line of spheres. The same characteristic pattern is evident in the confocal image (white dashed line) confirming that the square lattice seen in (a) arises from a NaCl rather than a CsCl structure.

is $\phi^*_{\mathrm{CsCl}}(\gamma) = \sqrt{3}\pi(1+\gamma^3)/[2(1+\gamma)^3]$. For $\gamma = 0.93$ the corresponding maximum volume fraction is $\phi^*_{\mathrm{CsCl}} = 0.68$, which indicates that the CsCl superlattice observed is dense packed and the particles are close to touching each other. Note that, although dense, the CsCl crystal is not a maximally packed structure. When the two particles A and B are identically sized, CsCl is isostructural with a bcc packing of spheres that fills space significantly less efficiently than fcc packing ($\phi_{\mathrm{fcc}} = 0.74$). Cesium chloride crystals were identified in binary samples with a wide range of volume fractions $0.507 \leq \phi \leq 0.578$. In each case CsCl growth always preceded initial formation of a substitutionally disordered random-stacked close-packed crystal.

A further increase in the charge on the two particles led to the formation of a third AB superlattice. Figure 3(a) shows a confocal micrograph of the superlattice formed 215 hours after mixing in a binary mixture of total volume fraction $\phi = 0.528$. Crystallographic modeling [Fig. 3(b)] reveals that the ordered regions visible are consistent with cleavage along the {100} and {111} (data not shown) planes of a NaCl superlattice (SG 225). The projection of the {100} plane visible in Fig. 3(a) is superficially similar to the {100} plane of the CsCl superlattice visible in Fig. 2(a). However, the two structures are easily discriminated by stepping the depth of focus. In the NaCl superlattice the vertically aligned columns of particles, visible in Fig. 3(b), are composed of alternating A and B particles in contrast to the CsCl structure [Fig. 2(b)]. The NaCl structure is most conveniently envisaged as two interpenetrating simple cubic lattices, occupied by an equal number of either sodium or chloride ions so that each ion has six unlike ions as its nearest neighbors. Analysis gave an average unit cell length a_{NaCl} of 3.3 ± 0.2 μm, which equates to a crystal volume fraction of $\phi_{\mathrm{NaCl}} = 0.49 \pm 0.09$. The maximum packing fraction of the NaCl superlattice is $\phi^*_{\mathrm{NaCl}}(\gamma) = 2\pi(1+\gamma^3)/[3(1+\gamma)^3]$ for a mixture of spheres with a size ratio $\gamma \geq \sqrt{2} - 1$. For $\gamma = 0.93$ this expression gives a maximum volume fraction of $\phi^*_{\mathrm{NaCl}} = 0.53$, which is in reasonable agreement with the value measured. The low packing fraction is readily understood if it is remembered that a NaCl crystal is equivalent to sc packing when no distinction is made between oppositely charged spheres. It is striking that NaCl is observed even though ϕ^*_{NaCl} is considerably lower than the maximum packing fractions of either CsCl ($\phi^*_{\mathrm{CsCl}} = 0.68$) or rhcp ($\phi^*_{\mathrm{rhcp}} = 0.74$).

The complex self-organization evident in our experiments is a consequence of a subtle interplay between entropy which favors dense close-packed structures and electrostatic interactions which prefer more open non-close-packed structures with reduced particle coordination. The same balance plays a fundamental role in the study of molten salts where it is frequently described in terms of the restricted primitive model (RPM). The RPM consists of a mixture of equal-sized hard spheres, half of which carry a positive charge and the remainder an equal but opposite negative charge to ensure charge neutrality. The ions i and j interact through a potential that is a sum of a hard-sphere

repulsion and a purely Coulombic term,

$$u_{ij}(r) = \begin{cases} \infty & \text{if } r < \sigma, \\ \pm u_c(\frac{\sigma}{r}) & \text{if } r \geq \sigma. \end{cases} \quad (1)$$

In Eq. (1), u_c is the magnitude of the Coulombic potential at contact, σ is the hard-sphere diameter, and the plus and minus signs apply, respectively, to interactions between ions of the same and different charges. The RPM is unlikely to be an accurate model of our experiments as it does not incorporate electrostatic screening. Nevertheless, the RPM accounts at least qualitatively for many of our observations.

The solid phases formed at high density in the restricted primitive model have been investigated by a number of authors, both theoretically [19,20] and more recently by Monte Carlo simulations [21,22]. The phase diagram is a function of ϕ and u_c/k_BT, the relative strength of the Coulombic potential at contact and the thermal energy. At low potentials $u_c \lesssim 3.5k_BT$, where hard-sphere repulsions dominate, a fluid phase of ions is predicted to freeze at a density $\phi \approx 0.5$ into a substitutionally disordered close-packed fcc crystal. The transition is driven by the higher entropy of the fcc crystal as compared to a fluid of the same density. Introducing Coulombic interactions adds potential as well as entropic contributions to the total free energy. In a purely random fcc structure each ion is surrounded by six ions of the opposite charge while in CsCl each ion has eight surrounding counterions. Consequently, we expect a fcc-CsCl transition as the Coulombic forces are increased. Computer simulations shows that the CsCl crystal is stabilized when $u_c \geq 4.3k_BT$. At high densities and charges the RPM predicts a further solid phase [22]. However, the structure is expected to be tetragonal rather than the cubic NaCl crystal observed here. Nonetheless, it is well known that, for a number of alkali-metal halides, the free energies of the CsCl and NaCl structures are sufficiently close that pressures of a few hundred kilobar are sufficient to interconvert the two structures. Consequently, our observation of NaCl may be a consequence of subtle differences in the interaction potential from the purely Coulombic mixture of oppositely charged spheres assumed in the RPM.

In summary, we have demonstrated how the introduction of a weak reversible attraction between equal-sized particles leads to a surprisingly complex solid phase behavior with observation of substitutionally disordered rhcp, CsCl, and NaCl binary crystals. Although to date we have explored only a single radius ratio ($\gamma = 0.93$), we have shown that a cross attraction between particles stabilizes several new non-close-packed structures, which are unstable in pure hard-sphere mixtures at the same size ratio. Our study suggests that competition between entropy and electrostatic interactions may provide a general route for the synthesis of new and more complex binary structures than can be stabilized by entropy alone and highlights the potential to direct the spontaneous growth of nanoparticles into a diverse range of superstructures by engineering the interactions between species.

Note added.—Recently we became aware of a study by Leunissen *et al.* [23] that shows similar effects in a system of *different-sized* colloidal spheres.

[1] J. V. Sanders, Philos. Mag. A **42**, 705 (1980).
[2] Y. A. Vlasov, X.-Z. Bo, J. C. Sturm, and D. J. Norris, Nature (London) **414**, 289 (2001).
[3] D. A. Mazurenko, R. Kerst, J. I. Dijkhuis, A. V. Akimov, V. G. Golubev, D. A. Kurdyukov, A. B. Pevtsov, and A. V. Sel'kin, Phys. Rev. Lett. **91**, 213903 (2003).
[4] J. H. Holtz and S. A. Asher, Nature (London) **389**, 829 (1997).
[5] M. D. Eldridge, P. A. Madden, and D. Frenkel, Nature (London) **365**, 35 (1993).
[6] E. Trizac, M. D. Eldridge, and P. A. Madden, Mol. Phys. **90**, 675 (1997).
[7] P. Bartlett, R. H. Ottewill, and P. N. Pusey, Phys. Rev. Lett. **68**, 3801 (1992).
[8] N. Hunt, R. Jardine, and P. Bartlett, Phys. Rev. E **62**, 900 (2000).
[9] A. B. Schofield, Phys. Rev. E **64**, 051403 (2001).
[10] F. X. Redl, K. S. Cho, C. B. Murray, and S. O'Brien, Nature (London) **423**, 968 (2003).
[11] A. E. Saunders and B. A. Korgel, Chem. Phys. Chem. **6**, 61 (2005).
[12] A. V. Tkachenko, Phys. Rev. Lett. **89**, 148303 (2002).
[13] A. Rugge and S. H. Tolbert, Langmuir **18**, 7057 (2002).
[14] V. T. Milam, A. L. Hiddessen, J. C. Crocker, D. J. Graves, and D. A. Hammer, Langmuir **19**, 10 317 (2003).
[15] A. I. Campbell and P. Bartlett, J. Colloid Interface Sci. **256**, 325 (2002).
[16] P. Royall, M. E. Leunissen, and A. van Blaaderen, J. Phys. Condens. Matter **15**, S3581 (2003).
[17] The total Br^- ion density is $\approx 30\ \mu m^{-3}$ and was calculated from measurements of the solvent conductivity and the charge on each particle. The electrostatic potential $u_{AB}(r)$ was evaluated from the DLVO expression,

$$\frac{u_{AB}(r)}{k_BT} = Z_AZ_B\left[\frac{\exp(\kappa(R_A + R_B))}{(1 + \kappa R_A)(1 + \kappa R_B)}\right]\frac{\lambda_B \exp(-\kappa r)}{r},$$

with a Bjerrum length $\lambda_B = 9$ nm.
[18] W. G. T. Kranendonk and D. Frenkel, Mol. Phys. **72**, 679 (1991).
[19] J.-L. Barrat, J. Phys. C **20**, 1031 (1987).
[20] C. Vega, F. Bresme, and J. L. F. Abascal, Phys. Rev. E **54**, 2746 (1996).
[21] B. Smit, K. Esselink, and D. Frenkel, Mol. Phys. **87**, 159 (1996).
[22] F. Bresme, C. Vega, and J. L. F. Abascal, Phys. Rev. Lett. **85**, 3217 (2000).
[23] M. E. Leunissen, C. G. Christova, R. van Roji, A. Imhof, and A. van Blaaderen, Nature (London) (to be published).